

## INFLOW PERFORMANCE OF COLD CO<sub>2</sub> INJECTION IN DEPLETED GAS FIELDS

**E. Peters<sup>1\*</sup>, D. Loeve<sup>1</sup>, S. Hurter<sup>1,2</sup>, F. Neele<sup>1</sup>**

<sup>1</sup> TNO, Utrecht, The Netherlands

<sup>2</sup> The University of Queensland, Brisbane, Australia

\* Corresponding author e-mail: lies.peters@tno.nl

### Abstract

Injection of CO<sub>2</sub> in depleted hydrocarbon fields often leads to differences in temperature between the injected CO<sub>2</sub> and the reservoir formation and fluids. A low pressure in the reservoir after depletion leads to decompression and cooling of the CO<sub>2</sub>. The temperature contrast can become significant, up to tens of degrees centigrade. For safe and efficient injection and storage of cold CO<sub>2</sub>, simulation of pressure and temperature in the pipelines, wells and reservoir is required. The reservoir is generally represented in a simplified way in pipeline and well models via multi-dimensional tables. A sensitivity analysis of CO<sub>2</sub> injection in a realistic reservoir model shows that for cold CO<sub>2</sub> injection below the critical pressure, such tables are too limited. The high variability in CO<sub>2</sub> properties (density and viscosity) makes the injectivity highly variable.

**Keywords:** CO<sub>2</sub> storage; Coupled models; Thermal CO<sub>2</sub> reservoir simulator; Well model

### 1. Introduction

Storage of CO<sub>2</sub> in the subsurface is seen as a viable option to reduce global warming, when it can be done in a safe and efficient way. A key element for the storage of carbon dioxide (CO<sub>2</sub>) are the injection wells, which bring the CO<sub>2</sub> from the high-pressure surface transport pipeline to the underground storage reservoir, such as a depleted gas field or saline aquifer. Accurate prediction of the pressure and temperature in the pipelines and wells during CO<sub>2</sub> injection is required for both operations and conformance monitoring. Conformance monitoring entails measuring wellhead and bottom hole conditions and comparing measured values with forecasts to ascertain that the integrity and safety of the storage site is maintained [1].

The CO<sub>2</sub> temperature at bottom hole is likely to be significantly lower than that of the storage formation. This temperature difference is caused by the fluid (CO<sub>2</sub>), which does not thermally equilibrate instantaneously with the geothermal gradient; especially at high flow rates a significant temperature difference is expected. The bottom hole conditions during injection depend on the conditions in the transport pipeline (pressure, temperature, CO<sub>2</sub> composition), the flow rate down the well, as well as on properties of the storage reservoir and the conditions in the reservoir near the well [4][9][10][11]. The latter are affected by the injection history.

The properties of the injection fluid – CO<sub>2</sub> fraction, density, viscosity – vary strongly over the pressure and temperature interval that is relevant for injection into depleted fields, especially when reservoir pressure and injection temperature is below the liquid-vapor phase line (lower than about 50 bar and 30 °C). Uncertainties in, for example, near-well pressure, temperature, saturation, and permeability may translate into relatively large

uncertainties in forecasts of bottom hole conditions and flow rates. The same is true for the condition at the well head. Large uncertainties in for example predicted bottom hole pressure and tubing head pressures are a problem for both operation planning and conformance monitoring.

For monitoring and risk management purposes it is important to quantify which conditions can't be explained by safe CO<sub>2</sub> injection, but are associated with certain risk factors (e.g. fracture propagation due to cold CO<sub>2</sub> around the well). A proper analysis is only possible with modelling tools that, on the one hand, take into account the direct coupling between the properties of CO<sub>2</sub> and the reservoir conditions and, on the other hand, the wellhead/bottom hole conditions of the CO<sub>2</sub> (e.g. Joule-Thomson effect in the reservoir and injection well, evaporation and dissolution) [2][4][5]. This requires the reservoir to be represented in the well and pipeline models. Mostly this is done using Inflow Performance Relationship (IPR) curves, which give inflow rate as a function of bottom hole and reservoir pressure. Because of the strong effect that temperature has, CO<sub>2</sub> injection simulations need to be coupled to heat transport to describe conditions at specific temperatures and pressures. Therefore, temperature is an additional parameter.

Due to the highly variable properties of the CO<sub>2</sub> at low pressure and low injection temperature, creating a set of IPR curves is not trivial, in particular with respect to temperature. Also these curves are limited because they do not include the effect of well interference and uncertainty.

This paper investigates the injectivity of cold CO<sub>2</sub> in depleted gas fields with the purpose of representing the reservoir in a well bore and network model. Sensitivity analysis is used to understand the dependence of

injectivity on injection rate and temperature and how to represent this for a well bore flow model. To ensure that the results are representative for actual depleted gas fields a realistic, multi-well reservoir model is used.

## 2. Approach

### 2.1 Model approach

To investigate the injectivity of CO<sub>2</sub> injection in a realistic depleted gas reservoir, a numerical modelling tool is used. The model is based on an existing gas field and has the following characteristics:

- A tilted fault block with moderately-sized aquifer
- The abandonment pressure is ~ 15 bar.
- The reservoir temperature is ~126 °C
- The field is first produced and then filled through three near-vertical wells.
- The main flow occurs in a high-permeability thin upper zone. Permeability decreases with depth.

To simulate the injection of cold CO<sub>2</sub>, it is important to accurately account for the physical processes in the reservoir. Joule-Thomson cooling and evaporation of formation water are accurately represented. However, to keep the numerical burden manageable in a sensitivity analysis some simplifications are made:

- The initial reservoir is filled with CO<sub>2</sub> instead of natural gas. Although the depletion phase is simulated for natural gas, before the start of the CO<sub>2</sub> injection, the remaining in-situ gas is changed to CO<sub>2</sub>. The impact of this simplification was checked and found to be negligible for the injectivity of the wells.
- To improve stability of the runs, instead of pure CO<sub>2</sub>, some CH<sub>4</sub> and water (3%) were added to the injection stream. This also changed the results very little.
- CO<sub>2</sub> dissolution and salt precipitation and chemical reactions are not included in these simulations.
- Non-Darcy flow is not included although it is known to occur for high rate CO<sub>2</sub> wells [7].

The impact of mechanical effects is not included, although they could significantly affect well injectivity. In particular, the reduction in temperature can lead to thermal stress fracturing of the formation [8]. Temperatures mostly remain high enough (> 10 °C) to avoid hydrate formation [5]. Also in real applications this will normally be avoided.

An important choice for the simulation is the grid size near the well. Instead of using single-well models to represent the near-well physics in detail, a multi-well model was used. Previous models studying the behaviour of cold CO<sub>2</sub> injection near the critical point were mostly single well models [2][3][5]. The main reason for using a multi-well model is to incorporate interference between

wells and the influence of reservoir architecture (faults and permeability heterogeneity).

The impact of three different grid sizes was evaluated. Table 1 gives the input settings. The results make it clear that for the case of 50 x 50 m grid blocks, the behaviour was averaged to such a degree that the conditions for Joule Thomson (JT) cooling were not well met. JT cooling is strongest for low pressure and temperature (see e.g. [4]). In coarse grids, the pressure has increased substantially before the near well area is sufficiently cold to cause a strong JT effect. JT cooling and vaporization could clearly be observed in the finest grid model and the temperature in the near well bore area dropped below injection temperature. Figure 1 shows the impact on the Bottom Hole Pressure (BHP) of the three different grid sizes for the same injection rate and injection temperature. This result shows that although the detailed behaviour is less well represented using coarse grid blocks, the overall behaviour doesn't change much, except in the first moments of injection and near the phase change. For the following simulations, the model with two levels of grid refinement were used.

Table 1: Approximate sizes of grid near the well. For the thickness in the vertical (dz) the values in the main reservoir are given.

	dx = dy	dz
No refinement	40 to 50 m	in main reservoir: ~4 m
1 level	20 to 25 m	in main reservoir: ~4 m
2 levels	10 to 12.5 m	in main reservoir: ~2 m

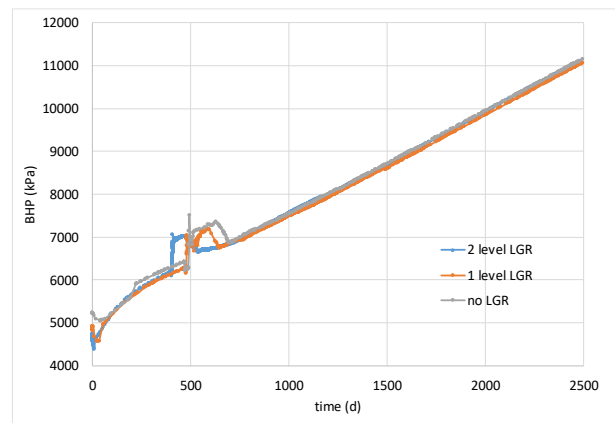


Figure 1: comparison of the impact of different near-well grid size (Table 1) on the BHP of the well for injection of 10 kg/s CO<sub>2</sub> at 15 °C.

### 2.2 Well injectivity

The Injectivity Index (II) is calculated to compare the behaviour of the well at different injection conditions. Although the definition of the injectivity index is very simple (injected mass rate divided by the pressure difference required to inject), in practice the difficulty is in defining the appropriate reservoir pressure that is used to estimate this pressure difference. In order to be appropriate for understanding the injectivity in relation to

a wellbore flow model, the reservoir pressure should represent the pressure ‘felt’ by the well. For comparison with observations, it should ideally be close to the reservoir pressure estimated from a well test.

Here, the average pressure in the area surrounding the well in the main reservoir layers is taken as the reservoir pressure for the calculation of the II. Low permeability layers beneath the main reservoir layers were not included, because the pressure in these layers lags considerably compared to the reservoir. For each well a sector surrounding each well was defined such that they do not overlap.

### 3. Results

#### 3.1 Injectivity Index

As discussed, the main reason for using a multi-well reservoir model, rather than single-well models with a detailed grid, is to be able to represent the interaction between wells. As we are not interested in the very fast transients at start-up of injection, output for the first two days was omitted. In Figure 2, the difference in injectivity is plotted for injection in a single well or all three wells. It is clear that the injectivity decreases significantly due to interference with other wells. This is expected because the reservoir is well connected and the wells are not very far apart. The distance between well 1 and the nearest other well is approximately 2 km.

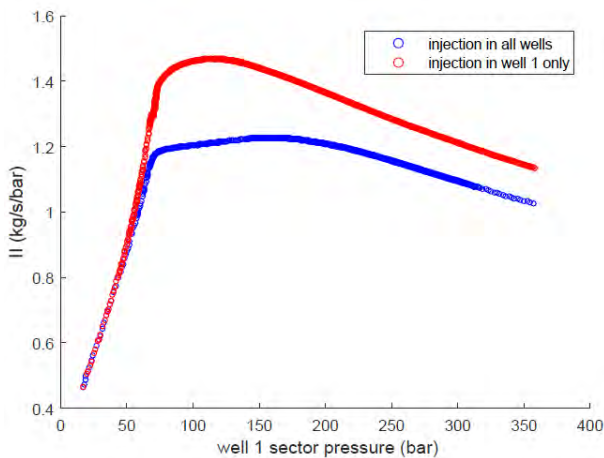


Figure 2: Difference in injectivity resulting from interference between wells (injection rate is 20 kg/s and injection temperature is 30 °C).

To investigate the impact of the injection rate and temperature a set of simulations was conducted with injection temperatures of 30, 45 and 60 °C and injection rates of 10 and 20 kg/s. The results are presented in Figure 3 and Figure 4. In Figure 3, the colour indicates the injection rate and in Figure 4 the colour indicates the injection temperature. Initially, the scenarios with the same rate have similar injectivity (Figure 3). In late time (or at higher pressure) on the other hand, the scenarios with the same injection temperature converge (Figure 4). The same behaviour was seen in the other wells (not presented here). To explain this behaviour, the properties of the CO<sub>2</sub> in the sector around the well are plotted in the

top figure of Figure 5 and the well bottom hole conditions in the underlying figure. Initially the density increases steeply due to the change in pressure. Since the injectivity is expressed in kg/s/bar, a higher density means a higher injectivity. In late time, the difference in viscosity due to the temperature difference dominates the difference in injectivity: the reservoir cools.

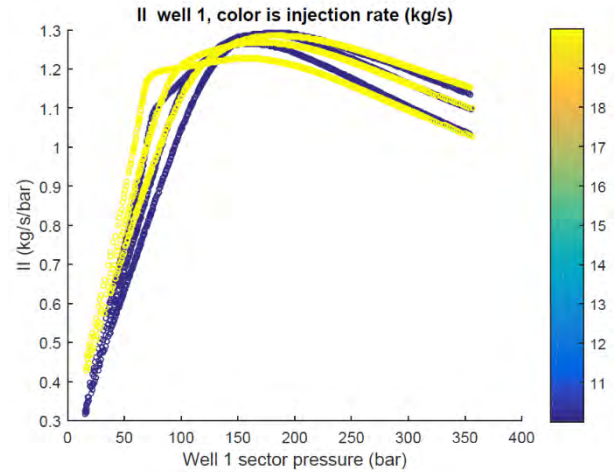


Figure 3: Injectivity index (kg/s/bar) for injection temperatures of 30, 45 and 60 °C and injection rates of 10 and 20 kg/s (indicated by colour) as a function of the well sector pressure.

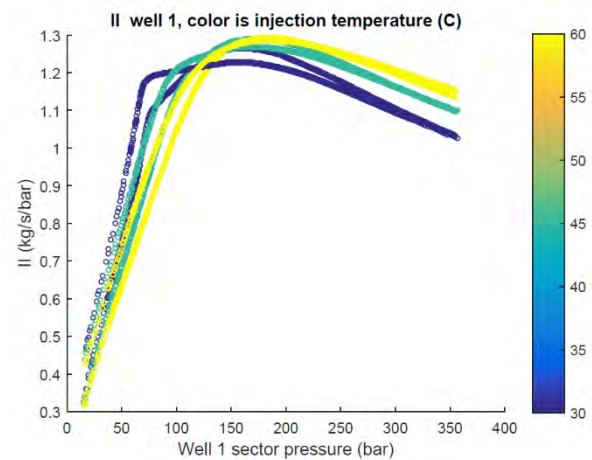


Figure 4: Injectivity index (kg/s/bar) for injection temperatures of 30, 45 and 60 °C (indicated by the colour) and injection rates of 10 and 20 kg/s as a function of the well sector pressure.

For the simulations so far, the range in injection rate and temperature was relatively small. For the initial injection period (up to a reservoir pressure of 100 bar), a more extensive range of injection rates and temperatures was simulated: 2 to 40 kg/s and 15 to 75 °C. The results are presented in Figure 6 and Figure 7. Now we can see that the range in injectivity increases considerably. The strong variations in injectivity around 40 bar are mainly caused by numerical instabilities, which can occur due to the strong changes in density and viscosity (Figure 5). Not all runs with an injection temperature of 15°C finished. For the high rate at 15°C, a more gradual ramping up of the rate would be required, but this was not conducted in this study.



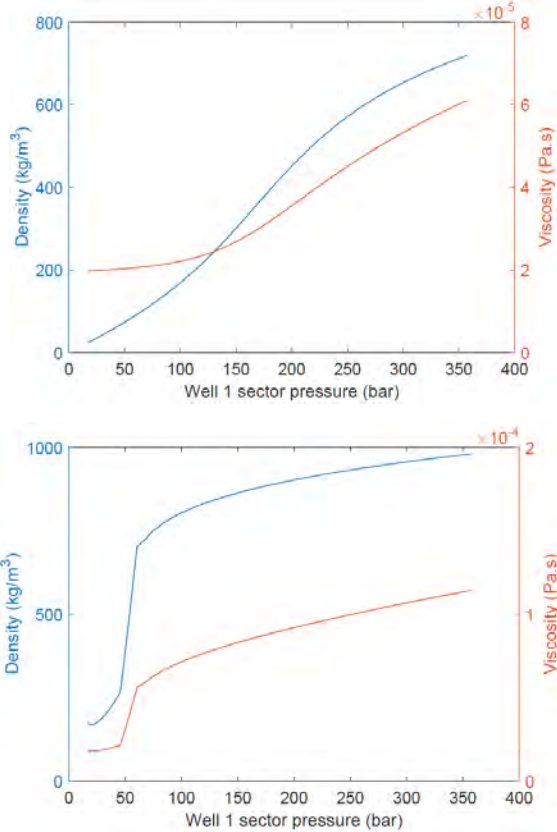


Figure 5: Properties of the CO<sub>2</sub> at average reservoir conditions in the sector around well 1 (top) and at well down hole conditions (bottom) for an injection rate of 20 kg/s and injection temperature of 30 °C.

From Figure 6, it is clear that initially the injection rate causes the largest span in injectivity. This can be understood from the CO<sub>2</sub> density and viscosity in the well which are plotted in Figure 8 and Figure 9. Injection at 15°C behaves differently than at higher temperatures because it is below the critical point. For all other injection temperatures, the impact on density and viscosity is larger for the rate than the temperature at low pressure.

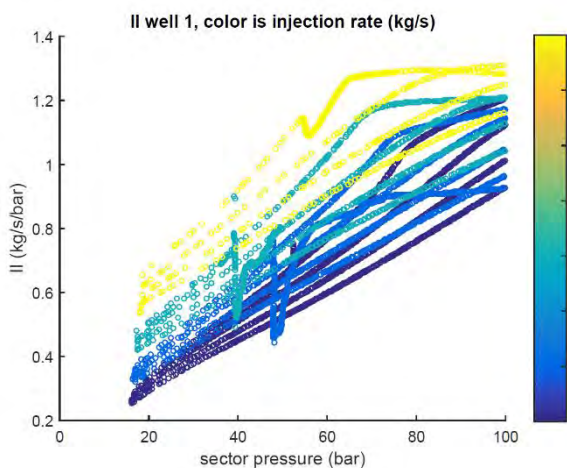


Figure 6: Injectivity Index II (kg/s/bar) for injection temperatures varying injection rate and temperature as a function of the well sector pressure (colour is injection rate).

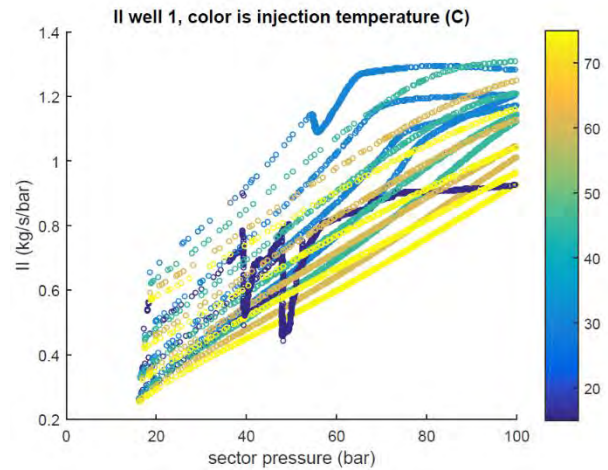


Figure 7: Injectivity Index II (kg/s/bar) for injection temperatures varying injection rate and temperature as a function of the well sector pressure (colour is injection temperature).

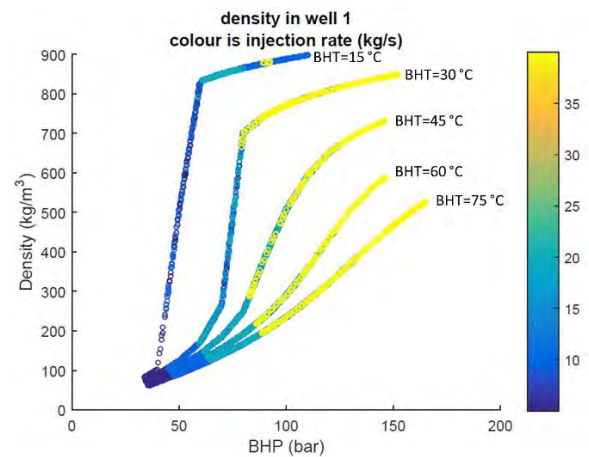


Figure 8: Density (kg/m<sup>3</sup>) in the well at down hole conditions as a function of bottom hole pressure (BHP) and bottom hole temperature (BHT).

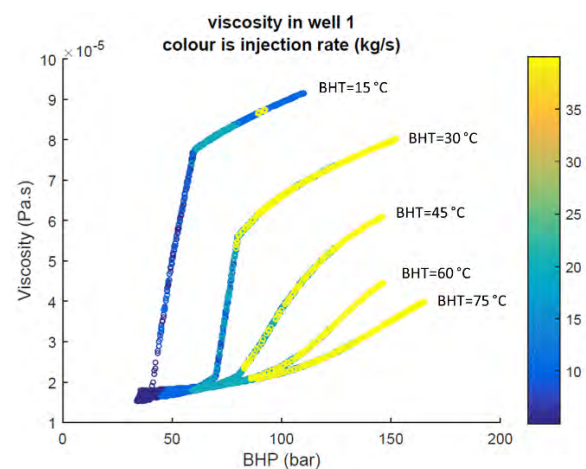


Figure 9: Viscosity (Pa.s) in the well at down hole conditions as a function of bottom hole pressure (BHP) and bottom hole temperature (BHT).

To reduce the large variability in the graphs due to the variability in density, the volumetric injectivity can be plotted instead of the mass injectivity used so far. This is similar to using a gas pseudo-pressure approach. The volumetric injectivity index is calculated by multiplying the mass rate by the CO<sub>2</sub> density at down hole conditions. The results in Figure 4 recalculated as volumetric injectivity index are plotted in Figure 10. Now the impact of temperature on injectivity is much more dominant, except at low pressure.

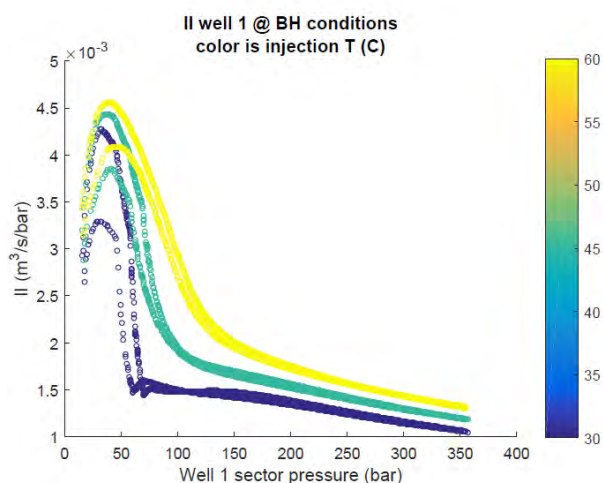


Figure 10: Volumetric Injectivity Index  $II$  ( $\text{m}^3/\text{s}/\text{bar}$ ) for injection temperatures of 30, 45 and 60 °C (indicated by the colour) and injection rates of 10 and 20 kg/s as a function of the well sector pressure.

These results show that if reservoir pressure and temperature are comfortably above the phase line, injection can be represented using a 4-dimensional IPR curves depending on reservoir and well pressure and temperature. However for lower temperature and pressure, such tables become unfeasible due to the high variability in the CO<sub>2</sub> properties. Since a full coupling of a multi-well model with well and pipeline models is currently not available and would be extremely demanding in terms of simulation effort and CPU time, a smarter solution needs to be developed. In the next step, we propose to use machine learning techniques to replace the tables for IPR curves. This will also allow to include the well interference in well-reservoir coupling.

#### 4. Summary and conclusions

In this paper, we presented a sensitivity analysis for injection of cold CO<sub>2</sub> in a realistic depleted low pressure

gas reservoir tapped by three wells. The variability of the injectivity index with changes in rate and temperature below the CO<sub>2</sub> critical pressure is very large and would be difficult to represent in tables. We examined only a limited number of relevant processes (JT cooling and evaporation). For accurate pipeline and well modelling, the reservoir should therefore be represented in a more comprehensive way than with multi-dimensional tables.

#### References

- [1] Steeghs Ph., Neele F., Gittins C., Ros, M., 2014, Drafting a monitoring plan for the ROAD project under the EU CCS Directive, Energy Procedia 63 ( 2014 ) 6680 – 6687.
- [2] Oldenburg, C.M. (2007) Joule-Thomson cooling due to CO<sub>2</sub> injection into natural gas reservoirs. Energy Conv. Manag. 48, p 1808-1815. Doi: 10.1016/j.enconman.2007.01.010
- [3] Ziabakhsh-Ganji, Z. and H. Kooi (2014) Sensitivity of Joule-Thomson cooling to impure CO<sub>2</sub> injection in depleted gas reservoirs. Applied Energy 113 434-451. Doi: dx.doi.org/10.1016/j.apenergy.2013.07.059.
- [4] Carniero, J.N.E., M.A. Pasqualetto, J.F.R. Reyes, E. Krogh, S.T. Johansen; J.R.P. Ciambelli, H.T. Rodrigues, R. Fonseca Jr. (2015) Numerical Simulations of High CO<sub>2</sub> Content Flows in Production Wells, Flowlines and Risers. OTC-26231-MS.
- [5] Voskov, D. V., Henley, H., & Lucia, L. (2017). Fully Compositional Multi-Scale Reservoir Simulation of Various CO<sub>2</sub> Sequestration Mechanisms. Computers & Chemical Engineering, 96(4), 183-195. doi: 10.1016/j.compchemeng.2016.09.021
- [6] Hoteit, H., M. Fahs and M. R. Soltanian (2019) Assessment of CO<sub>2</sub> Injectivity During Sequestration in Depleted Gas Reservoirs. Geosciences 9. doi:10.3390/geosciences9050199.
- [7] Grigg, R.B., Z. Zeng and L.V. Bethapudi, 2004. Comparison of Non-Darcy flow of CO<sub>2</sub> and N<sub>2</sub> in a carbonate rock. SPE 89471.
- [8] Salimzadeh, S., Paluszny, A., Zimmerman, R.W. (2018) Effect of cold CO<sub>2</sub> injection on fracture apertures and growth, IJGGC 74, 130-141
- [9] Paterson, L., J. Ennis-King, S. Sharma (2010) Observations of Thermal and Pressure Transients in Carbon Dioxide Wells. SPE134881.
- [10] Böser, W. and S. Belfroid (2013) Flow Assurance Study. GHGT-1. Energy Procedia 37, 0.1016/j.egypro.2013.06.188.
- [11] Veltin, J. and S. Belfroid 2012. Dynamics of CO<sub>2</sub> Transport and Injection Strategies in a Depleted Gas Field. CMTC-151265.